Inorg. Chem. **2008**, *47*, 10771−10778

Functional Evaluation of Iron Oxypyriporphyrin in Protein Heme Pocket

Saburo Neya,*,† Masaaki Suzuki,† Hirotaka Ode,† Tyuji Hoshino,† Yuji Furutani,‡ Hideki Kandori,‡ Hiroshi Hori,§ Kiyohiro Imai,|| and Teruyuki Komatsu⊥,#

Department of Physical Chemistry, Graduate School of Pharmaceutical Sciences, Chiba University, Inage-Yayoi, Chiba 263-8522, Japan, Department of Material Science and Engineering, Nagoya Institute of Technology, Showa-ku, Nagoya 466-8555, Japan, Division of Biophysical Engineering, Graduate School of Engineering Science, Osaka University, Toyonaka, Osaka 560-8531, Japan, Department of Material Chemistry, Faculty of Engineering, Hosei University, Koganei, Tokyo 184-8787, Japan, Research Institute for Science and Engineering, Waseda University, Okubo, Shinjuku, Tokyo 169-8555, Japan, and PRESTO JST, Okubo, Shinjuku, Tokyo 169-8555, Japan

Received July 26, 2008

The iron complex of oxypyriporphyrin, a porphyrinoid containing a keto-substituted pyridine, was coupled with apomyoglobin. The reconstituted ferric myoglobin was found to be five-coordinate without iron-bound water molecules. The anionic ligands such as CN^- and N_3^- bound the myoglobin with high affinities, while neutral imidazole did not. The IR observation indicated that the azide complex was pure high-spin, although the corresponding native protein was in the spin-state equilibrium. The reduced myoglobin was five-coordinate but exhibited no measurable affinity for O_2. The affinity for CO was lowered down to 1/2400 as compared with native myoglobin. These anomalies were ascribed to the deformation in the iron coordination core after the replacement of one of the four pyrroles with a larger pyridine ring. The ligand binding analyses for the ferric and ferrous myoglobin suggest that the proximal histidine pulls the iron atom from the deformed core to reduce the interaction between the iron and exogenous ligands. Similarity of the reconstituted myoglobin with guanylate cyclase, a NO-responsive signaling hemoprotein, was pointed out.

Introduction

Integrated globin−heme interactions are essential for the regular function of hemoproteins. The three important roles of the globin are to accommodate the heme, enhance the coordination of the proximal histidine, and inhibit the oxidation of the ferrous heme iron. Heme is a chromophore molecule where the pyrroles are lined up in a square arrangement. Recent advances in porphyrin synthesis allow us to rearrange artificially the tetrapyrrole over the porphyrin ring. The first example is porphycene, discovered by Vogel et al. in 1986.[1] Subsequent to Vogel et al.'s discovery of porphycene, other important porphyrin isomers of corrphycene and hemiporphycene were prepared.[2] These modified tetrapyrroles have characteristic molecular shapes: porphycene, corrphycene, and hemiporphycene are rectangular, trapezoidal, and asymmetric quadrate, respectively, while porphyrin is square.[2]

Oxypyriporphyrin (OxyPyP) is another kind of core-modified porphyrinoid where one of the pyrrole rings is replaced with a pyridine unit (Scheme 1). A nickel complex of this porphyrinoid was originally reported in 1993 by Bonnett's group,[3,4] but the first ring synthesis was published in 1996 by Lash and Chaney.[5] A number of synthetic and spectroscopic investigations on OxyPyP were subsequently reported.[6,7]

Owing to the keto group on the pyridine ring, the porphyrinoid is fully aromatic and exhibits an intense Soret band.[3−7] Pyridine, a six-membered analog of pyrrole, is formally obtained after a single carbon insertion to the pyrrole core and characterized with a $C_2-N_1-C_6$ bond

* Author to whom correspondence should be addressed. E-mail: sneya@p.chiba-u.ac.jp.
† Chiba University.
‡ Nagoya Institute of Technology.
§ Osaka University.
|| Hosei University.
⊥ Waseda University.
PRESTO JST.

(1) Vogel, E.; Köcher, M.; Schmickler, H.; Lex, J. *Angew. Chem., Int. Ed. Engl.* **1986**, *25*, 257–259.
(2) Sessler, J. L.; Gebauer, A.; Vogel, E. In *The Porphyrin Handbook*; Kadish, K. M., Smith, K. M., Guilard, R., Eds.; Academic Press: San Diego, CA, 2000; Vol. 2, pp 1−54.
(3) Adams, K. R.; Bonnett, R.; Burke, P. J.; Saigado, A.; Vallés, M. A. *Chem. Commun.* **1993**, 1860–1861.
(4) Adams, K. R.; Bonnett, R.; Burke, P. J.; Saigado, A.; Vallés, M. A. *J. Chem. Soc., Perkin Trans. 1* **1997**, 1769–1772.
(5) Lash, T. D.; Chaney, S. T. *Chem.—Eur. J.* **1996**, *2*, 944–948.

10.1021/ic801406x CCC: $40.75
Published on Web 10/10/2008

Scheme 1. Structure of the Iron Complex of OxyPyP Used in This Work

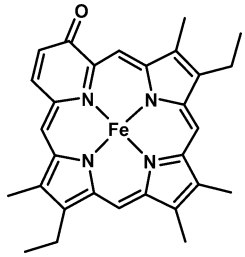

angle of 116.7° and a C_2-C_6 distance of 2.281 Å.[8] The corresponding molecular dimensions in pyrrole are 108.9° ($C_2-N_1-C_5$) and 2.250 Å (C_2-C_5).[8] Incorporation of a relatively bulky pyridine ring into porphyrin will deform the N_4-coordination core. The core deformation by pyridine could be comparable with that induced by the tetrapyrrole rearrangement in porphycene, corrphycene, and hemiporphycene.[2] Pyridine-containing OxyPyP is accordingly expected to exhibit intriguing properties as the three porphyrinoids do.

Although OxyPyP and the related macrocycles form stable transition-metal derivatives,[3,4,7,9] the iron compound has been scarcely analyzed. Eguchi et al. very recently indicated that the bis-coordinated 1-methylimidazole (1-MeIm) complex of OxyPyPFe(III) is of intermediate spin with $S = 3/2$, in marked contrast with the pure low-spin ($S = 1/2$) state in the regular heme.[10] OxyPyPFe(III) has been so far uncharacterized as a prosthetic group of hemoprotein because it has no direct biological relevance. However, the unique molecular structure of OxyPyP infers that the iron complex, when placed in a protein pocket, would seriously perturb biological functions. The objective of this work is to assess the relationships between the coordination structure in OxyPyP and the iron reactivity, and to pursue the functional consequence of hemoprotein. We report herein the first characterization of the iron porphyrinoid as the prosthetic group of myoglobin (Mb).

Materials and Methods

Macrocycle and Iron Complex. An OxyPyP, 9,18-diethyl-8,13,14,19-tetramethylpyriporphyrin in Scheme 1, was used throughout the work. The macrocycle was prepared by coupling 2,5-bis[(5-carboxy-3-ethyl-4-methylpyrrol-2-yl)methyl]-3,4-dimethylpyrrole and 3-hydroxy-2,6-pyridinedicarboxaldehyde as previously reported.[5,6] The crude product was purified with silica-gel column chromatography (eluent: $CHCl_3$/MeOH 20:1 v/v) before crystallization from chloroform/methanol (yield, 47%). Anal. calcd for $C_{29}H_{30}N_4O$; C, 77.30; H, 6.71; N, 12.43. Found: C, 77.53; H, 6.85; N, 12.20. ^{1}H NMR (400 MHz, $CDCl_3$, δ): 11.86 (s, 1H, *meso*-H), 9.52 (s, 1H, *meso*-H), 9.48 (s, 1H, *meso*-H), 9.32 (s, 1H, *meso*-H), 9.17 (d, 1H, $J = 7$ Hz, pyridine-H), 7.90 (d, 1H, $J = 7$ Hz, pyridine-H), 3.97 (m, 4H, 2 × $-CH_2CH_3$), 3.62 (s, 6H, ring $-CH_3$), 3.46 (s, 6H, ring $-CH_3$), 3.34 (s, 6H, ring $-CH_3$), 1.78 (m, 6H, 2 × $-CH_2CH_3$), −3.97 (br s, 1H, NH), −4.01 (br s, 1H, NH). MS: *m*/*z* 450 (M^+). Visible (chloroform) [λ_{max}, nm, (ε_{mM})]: 421 (142), 439 (74.1), 540sh (6.1), 548sh (6.4), 588 (20.1), 602sh (16.3), 609 (19.2), 659 (1.2). Iron was inserted into the macrocycle with the Adler method to afford the ferric chloride complex.[11]

Myoglobin Reconstitution. Sperm whale Mb was purchased from Sigma (type II). ApoMb was prepared with the method of Teale.[12] OxyPyPFe(III)Cl without the acid side chains was coupled with apoMb according to the same procedure as used for eitoporphyrinFe(III).[13] The crude Mb was purified on a CM-cellulose column (Whatman, CM-52) with a linear gradient of Tris buffer, 20−150 mM at pH 7.0, in a cold room. The dark fractions of Mb with an absorbance ratio of $A_{Soret}/A_{280\ nm} > 1.5$ were collected. The yield for the protein reconstitution was 80% or better.

Physical Measurements. Visible absorption spectra were recorded on a Shimadzu MPS-2000. IR spectra were obtained on a Nicolet Avatar spectrometer with an Oxford cooling unit at 2 cm^{-1} resolution with a 50 μm cell and apodized with a Happe-Genzel function. The X-band electron paramagnetic resonance (EPR) spectra were recorded with a Varian E12 spectrometer with a 100 kHz modulation (0.5 mT). Proton NMR spectra at 400 MHz were measured with a JEOL α400 spectrometer.

Ligand Binding. The ligand binding constants were spectrophotometrically determined and analyzed with the Benesi-Hildebrand equation.[14] The equilibrium CO affinity to the deoxy Mb was evaluated by optical titration of a CO saturated buffer in 0.1 M Tris at pH 7.0, as described by Sono et al.[15] The laser flash photolysis for the CO binding was carried on a Unisoku TSP-1000WK time-resolved spectrophotometer with a Spectron Laser System SL803G-10 Q-switched Nd:YAG laser, which generated a second-harmonic (532 nm) pulse of 6 ns duration (10 Hz).[16] The oxygen affinity to ferrous Mb in a 0.1 M phosphate buffer, pH 7.0, was measured on the automatic recording apparatus[17] in the presence of an enzymic reducing system.[18] All of the measurements were carried out at 20 °C.

Quantum Chemical Calculations. The molecular geometries of OxyPyPFe(III)Cl and porphineFe(III)Cl were optimized by quantum chemical calculations with the Gaussian 03 program.[19]

(6) Schnemeier, T.; Breitmeier, E. *Synthesis* **1997**, 273–275.
(7) Liu, D.; Ferrence, G. M.; Lash, T. D. *J. Org. Chem.* **2004**, *69*, 6079–6093.
(8) Acheson, R. M. *An Introduction to the Chemistry of Heterocyclic Compounds*; Interscience Publishers: New York, 1960; Chapters 3 and 5.
(9) Lash, T. D. In *The Porphyrin Handbook*; Kadish, K. M., Smith, K. M., Guilard, R., Eds.; Academic Press: San Diego, CA, 2000; Vol. *2*, pp 125−199.
(10) Eguchi, H.; Ohgo, Y.; Ikezaki, A.; Neya, S.; Nakamura, M. *Chem. Lett.* **2008**, *37*, 768–769.
(11) Adler, D.; Longo, F.; Kampas, F.; Kim, J. *J. Inorg. Nucl. Chem.* **1970**, *32*, 2443–2445.
(12) Teale, F. W. J. *Biochim. Biophys. Acta* **1959**, *35*, 543.
(13) Neya, S.; Funasaki, N.; Imai, K. *Biochim. Biophys. Acta* **1989**, *996*, 226–235.
(14) Benesi, H. A.; Hildebrand, J. H. *J. Am. Chem. Soc.* **1949**, *71*, 2703–2707.
(15) Sono, M.; Smith, P. D.; McCary, J. A.; Asakura, T. *J. Biol. Chem.* **1976**, *251*, 1418–1426.
(16) Komatsu, T.; Ohmichi, N.; Nakagawa, A.; Zunszain, P. A.; Curry, S.; Tsuchida, E. *J. Am. Chem. Soc.* **2005**, *127*, 15933–15942.
(17) Imai, K. *Methods Enzymol.* **1981**, *76*, 438–449.
(18) Hayashi, A.; Suzuki, T.; Shin, M. *Biochim. Biophys. Acta* **1973**, *310*, 309–316.
(19) Frisch, M. J.; Trucks, G. W.; Schlegel, H. B.; Scuseria, G. E.; Robb, M. A.; Cheeseman, J. R.; Montgomery, J. A., Jr.; Vreven, T.; Kudin, K. N.; Burant, J. C.; Millam, J. M.; Iyengar, S. S.; Tomasi, J.; Barone, V.; Mennucci, B.; Cossi, M.; Scalmani, G.; Rega, N.; Petersson, G. A.; Nakatsuji, H.; Hada, M.; Ehara, M.; Toyota, K.; Fukuda, R.; Hasegawa, J.; Ishida, M.; Nakajima, T.; Honda, Y.; Kitao, O.; Nakai, H.; Klene, M.; Li, X.; Knox, J. E.; Hratchian, H. P.; Cross, J. B.; Bakken, V.; Adamo, C.; Jaramillo, J.; Gomperts, R.; Stratmann, R. E.; Yazyev, O.; Austin, A. J.; Cammi, R.; Pomelli, C.; Ochterski, J. W.; Ayala, P. Y.; Morokuma, K.; Voth, G. A.; Salvador, P.; Dannenberg, J. J.; Zakrzewski, V. G.; Dapprich, S.; Daniels, A. D.; Strain, M. C.; Farkas, O.; Malick, D. K.; Rabuck, A. D.; Raghavachari, K.; Foresman, J. B.; Ortiz, J. V.; Cui, Q.; Baboul, A. G.; Clifford, S.; Cioslowski, J.; Stefanov, B. B.; Liu, G.; Liashenko, A.; Piskorz, P.; Komaromi, I.; Martin, R. L.; Fox, D. J.; Keith, T.; Al-Laham, M. A.; Peng, C. Y.; Nanayakkara, A.; Challacombe, M.; Gill, P. M. W.; Johnson, B.; Chen, W.; Wong, M. W.; Gonzalez, C.; Pople, J. A. *Gaussian 03*; Gaussian, Inc.: Wallingford CT, 2004.

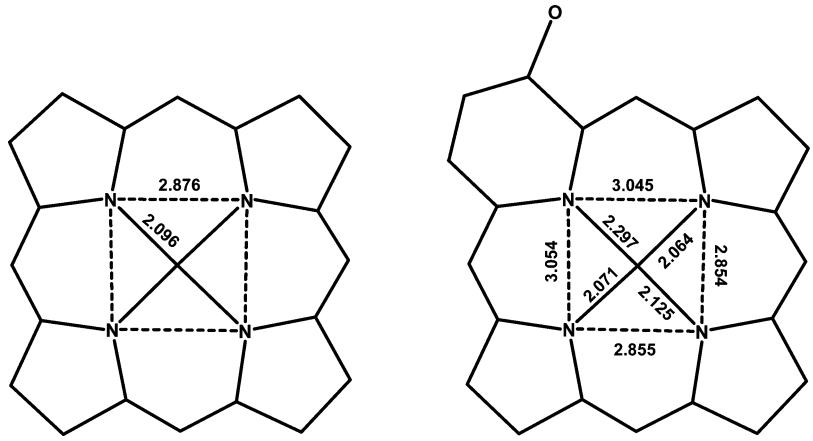

Figure 1. Formal diagram of the five-coordinate Fe(III)Cl complexes of porphine (left) and OxyPyP (right) obtained from the structural optimization with the quantum chemical calculation. The numerals are in angstroms. The axial Cl is omitted for clarity. The Fe−Cl distances are 2.230 and 2.218 Å for porphine and OxyPyP, respectively. The iron is displaced from the mean N_4 plane toward the Cl by 0.508 Å (porphine) or 0.483 Å (OxyPyP). Calculation was carried out for the macrocycles without peripheral chains.

The B3LYP/6-311++G** level was applied to the calculation, and the potential energy of the optimized structure was estimated at the same level of the theory.

Results

Prosthetic Group. We first characterized OxyPyP and the iron complex before going into the Mb complex. The spectrophotometric titration of free base OxyPyP in aqueous 2.5% sodium dodecyl sulfate was carried out to calculate the pK_3 value of the macrocycle because the value is important to estimate the properties of the core nitrogen atoms.[20] When the OxyPyP solution was acidified from pH = 7.4 to 1.9 with successive addition of dilute hydrochloric acid, the absorbance at 590 and 645 nm decreased and increased, respectively, with isosbestic points at 573, 586, and 629 nm (results not shown). Analysis of the 641 nm absorption decrease afforded a p$K_3 = 3.88 \pm 0.09$.

The pyridine hemochromogen spectrum[20] was characterized to determine the reconstituted Mb. A minimum amount of aqueous sodium dithionite was added to the OxyPyPFe(III)Cl dissolved in pyridine/dimethylformamide (1:1 v/v). The visible spectrum of ferrous OxyPyPFe(II)·bis(pyridine) was as follows: 436 nm (127 mM^{-1} cm^{-1}), 454 (84.9), 537sh (10.8), 569sh (14.5), 581 (18.5), and 604 (40.6). On the basis of the spectrum, the extinction coefficient of the Soret band, $\varepsilon_{429\ nm} = 93$ mM^{-1} cm^{-1}, was determined for the ferric Mb reconstituted with OxyPyPFe(III). We further characterized the hemochromogen spectrum of the bis-1-MeIm complex of OxyPyPFe(II) in a 1-MeIm/dimethylformamide (1:1, v/v) mixture to refer to the coordination state of the ferrous Mb. The absorption maxima of the bis-1MeIm complex of OxyPyPFe(II) were found at 438 nm ($\varepsilon = 121$ mM^{-1} cm^{-1}), 544sh (14.3), 571 (15.9), 586 (17.6), and 609 (34.0).

Figure 1 shows the calculated molecular structures of OxyPyPFe(III)Cl and porphineFe(III)Cl, which were optimized with a quantum chemical calculation. In porphineFe(III)Cl, the N_4 metallocore is square with a N−N distance of 2.876 Å, and the Fe−N(pyrrole) bond length is 2.096 Å. The Fe atom is displaced from the mean N_4 plane by 0.508 Å. These parameters are comparable with the those found for five-coordinate Fe(III) porphyrins,[21] suggesting the reliability of the calculation. The N_4 core in OxyPyPFe(III)Cl, on the other hand, is distorted to a rhomboid where the two sets of the N−N distances are 3.045 Å and 2.854 Å. Accordingly, OxyPyP has a larger N_4 core (8.708 $Å^2$) than porphineFe(III)Cl (8.271 $Å^2$). The four Fe−N bonds in the OxyPyPFe(III) are nonequivalent; the Fe−N(pyridine) bond (2.297 Å) is significantly longer than the Fe−N(pyrrole) bonds (2.125, 2.071, and 2.064 Å). The three Fe−N(pyrrole) bonds are comparable with or slightly longer than the 1.97−2.09 Å found in ordinary high-spin Fe(III) porphyrins.[21] On the other hand, the Fe−N(pyridine) bond (2.297 Å) in OxyPyPFe(III) is much longer than those (2.03−2.09 Å) in axially coordinating pyridines to low-spin Fe(III) and comparable with the 2.316 Å of 4-chloropyridine that is weakly coordinating to the high-spin Fe(III) porphyrin.[21] Thus, OxyPyP has an enlarged and deformed core when compared with porphyrin.

Binding of 1-Methylimidazole. We examined the binding of 1-MeIm to the OxyPyPFe(III). Figure 2 illustrates the visible absorption transition of OxyPyPFe(III)Cl during the 1-MeIm titration in an organic solvent. At low concentrations of the ligand up to 450 μM, the absorbance around 420 nm increased with clear isosbestic points at 407 and 464 nm. These isosbestic points were broken with the further addition of 1-MeIm, 0.50−15.8 mM. The results indicate that the 1-MeIm ligation proceeds in two steps through appreciable accumulation of the mono-1-MeIm adduct. From the analysis of the first absorbance changes with the plots of (1/[1-MeIm], 1/ΔA),[14] we obtained the binding constant $K_1 = 5900 \pm 230$ M^{-1}. The second binding process was analyzed with eq 1:[22,23]

$$\frac{A - A_0}{A[\text{1-MeIm}]^2} + \frac{(A - A_1)K_1}{A[\text{1-MeIM}]} = K_1K_2A_2(1/A) - K_1K_2 \quad (1)$$

We obtained the second association constant $K_2 = 197 \pm 27$ M^{-1}. The results indicating $K_1 \gg K_2$ is in contrast with

(20) Antonini, E.; Brunori, M. *Hemoglobin and Myoglobin in their Reactions with Ligands*; North Holland Publishing Company: Amsterdam, 1971; pp 10, 43−48.

(21) Scheidt, W. R.; Gouterman, M. In *Iron Porphyrins*; Lever, A. B. P., Gray, H. B., Eds.; Addison-Wesley Publishing. Co.: London, 1988; Part I, pp 89−139.

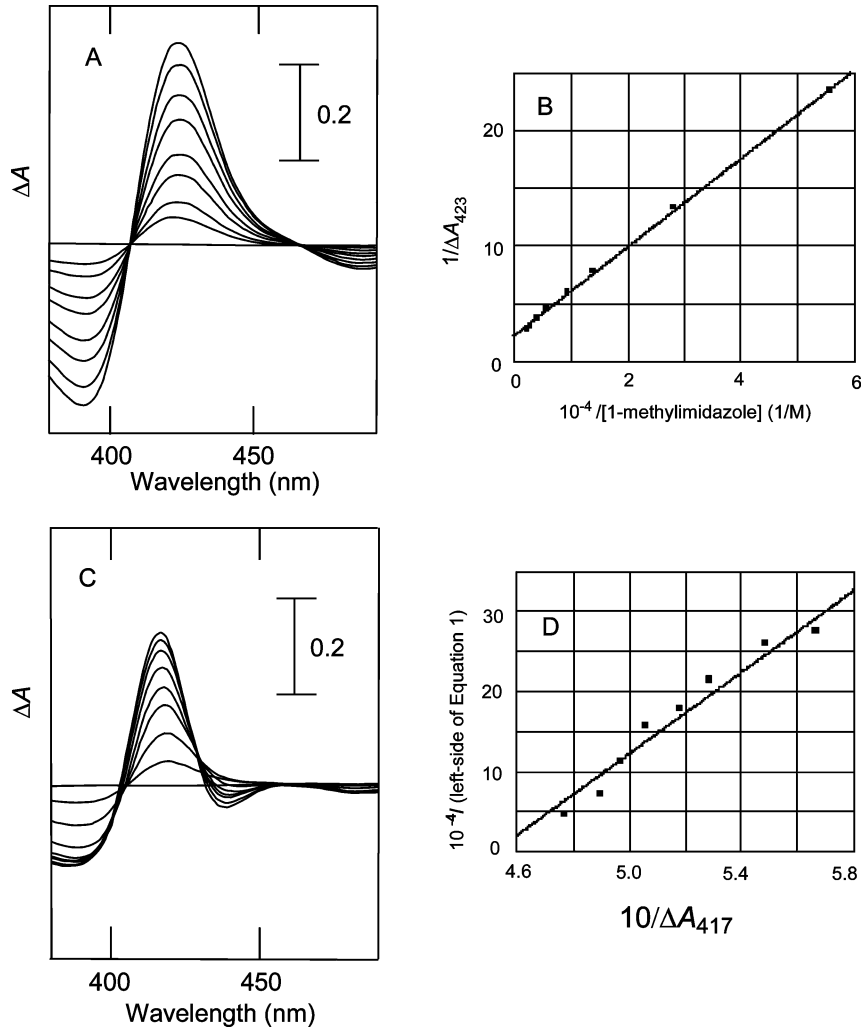

Figure 2. Optical titration of 1-methylimidazole to OxyPyPFe(III)Cl in dichloromethane at 20 °C. (A) Absorption changes in [1-methylimidazole] = 0−466 μM. (B) Analysis of the absorption changes at 423 nm. The first binding constant $K_1 = 5.92 \times 10^3$ M^{-1} was obtained. (C) Absorption changes in [1-methylimidazole] = 0.47−15.9 mM. (D) Analysis of the absorption changes at 417 nm. The second binding constant $K_2 = 197$ M^{-1} was obtained.

the tendency of $K_1 \ll K_2$ found in ordinary Fe(III) porphyrin,[24] demonstrating the stability of the mono-1-MeIm species.

Ferric Myoglobin. The spectrophotometirc titration of apoMb with OxyPyPFe(III) indicated a reflection point at a 1:1 stoichiometry. Figure 3 shows the light absorption spectrum of the Mb reconstituted with OxyPyPFe(III). The Soret band is at 429 nm, and dominant peaks occurred at 544, 610, and 657 nm. The visible sorption spectrum is dissimilar to that of native aquomet Mb with peaks at 405, 500, and 631 nm.[20] In Figure 3B, the EPR spectrum of the reconstituted Mb is provided. The reconstituted Mb at 5 K exhibited a main signal with $g = 4.34$ and minor peaks at $g = 8.97$, 8.16, and 7.41. The intensity of the $g = 8.97$, 8.16, and 7.41 signals are in marked contrast (to ca. 30%) at 15 K. The EPR profile, like the visible absorption, is dissimilar to that of native Mb. The spectrum is rather similar to those of the high-spin Fe(III) in transferrin, siderophore, and protocatecuate dioxygenase[25] and suggests a low-symmetric environment for the high-spin Fe(III) in OxyPyP.

The reconstituted Mb is capable of binding various anionic ligands. The azide titration caused a Soret peak shift from 429 to 435 nm, and we obtained a binding constant of $(6.16 \pm 0.17) \times 10^5$ M^{-1} (Figure 4). Other anionic ligands such as CN^-, F^-, OCN^-, and SCN^- bound to the Mb with high affinities. The visible spectra of the Mb derivatives and the binding constants are summarized in Figure 4 and Table 1. On the other hand, a neutral ligand imidazole did not cause the spectral change even at 1 M, and the imidazole ligation was not evidenced. Another notable result was that the spectrum of the ferric Mb was invariant over a range of pH 6−10. This is in contrast with native ferric Mb that exhibits notable spectral transition associated with the pH.[20]

IR of the Azide Complex. Azide is a high-affinity ligand to ferric hemoproteins. The azide complex is in an equilibrium between the high- ($S = 5/2$) and low-spin ($S = 1/2$)

(22) Rossotti, F. J. C.; Rossotti, H. *The Determination of Stability Constants*; McGraw Hill: New York, 1961; p 277.
(23) Neya, S.; Hoshino, T.; Hata, M.; Funasaki, N. *Chem. Lett.* **2004**, *33*, 114–115.
(24) Yoshimura, T.; Ozaki, T. *Bull. Chem. Soc. Jpn.* **1979**, *52*, 2268–2275.
(25) Bou-Abdallah, F.; Chasteen, N. D. *J. Biol. Inorg. Chem.* **2008**, *13*, 15–24.

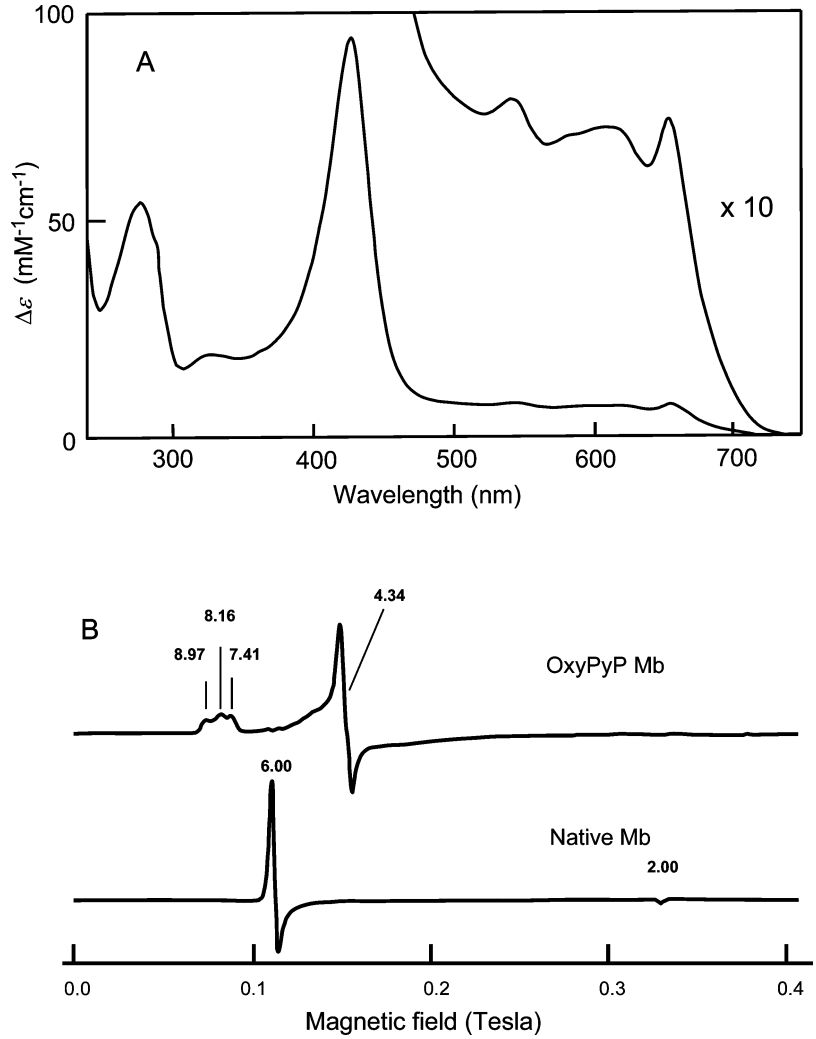

Figure 3. The ferric Mb reconstituted with OxyPyPFe(III). (A) UV−visible absorption spectra in 0.1 M Tris at pH 7.0 and 20 °C. (B) X-band EPR spectra of the reconstituted Mb (upper) and native Mb (lower) in 0.1 M Tris at pH 7.0 and 5 K.

states.[26] The antisymmetric stretching IR band of the iron-bound azide frequently splits into two peaks to reflect the spin-state equilibrium.[27,28] We recorded the IR spectra of the ferric azide Mb and the model complex to elucidate the coordination environment of the OxyPyPFe(III) in Mb. Figure 5 shows the IR spectra of the iron-bound azide in the model and Mb. The six-coordinate model, OxyPyPFe(III)·N_3^-·1-MeIm, was prepared by adding one equivalent of 1-MeIm to five-coordinate OxyPyPFe(III)·N_3^-.[28] The similar peak positions suggest a common coordination structure between the two systems. There are two additional observations in Figure 5. First, the Mb and OxyPyPFe(III) exhibit only single peaks at 2047 and 2049 cm^{-1}, respectively. This is in marked contrast with native Mb, which exhibits two azide bands around 2047−2043 cm^{-1} ($S = 5/2$, high-spin band) and 2023−2016 cm^{-1} ($S = 1/2$, low-spin band) to reflect the spin equilibrium.[26] The single IR band appeared at 2049 cm^{-1}, indicating that the Mb is pure high-spin. Another notable result is that the IR spectrum of the Mb is temperature-independent over a 260−300 K range (results not shown), unlike native Mb, which shows marked IR spectral transition with the temperature.[26]

Ferrous Myoglobin. The ferric Mb was readily reduced with a small amount of sodium dithionite or an enzymic reducing system to afford stable ferrous Mb. The solution changed from dark green to pale green upon reduction. Figure 6 illustrates the visible absorption spectra of the ferrous deoxy and CO Mb's.

Figure 7 provides the Soret optical changes of the deoxy Mb with the addition of CO. We obtained a CO affinity of $K_{CO} = (9.9 \pm 1.0) \times 10^3\ M^{-1}$ ($P_{50} = 74 \pm 7$ mmHg) at 20 °C. The affinity is only 1/2200 of the corresponding value $K_{CO} = 2.2 \times 10^7\ M^{-1}$ ($P_{50} = 0.033$ mmHg) for native Mb.[29] We examined the CO binding kinetics with flash photolysis to analyze the kinetic profile (Figure 7). The flash photolysis of the CO Mb afforded an apparent relaxation rate $k_{app} = 233\ s^{-1}$. With k_{app} and the equilibrium affinity K_{CO}, the association and dissociation constants were calculated to be $k_{on} = 2.0 \times 10^5\ M^{-1}\ s^{-1}$ and $k_{off} = 21\ s^{-1}$. On the other hand, the kinetic constants for the CO binding in native Mb are $k_{on} = 5.1 \times 10^5\ M^{-1}\ s^{-1}$ and $k_{off} = 1.9 \times 10^{-2}\ s^{-1}$.[29]

The oxygen binding profile of the ferrous Mb was entirely anomalous. Interestingly, when the ferric Mb was reduced with sodium ascorbate or the enzymatic system,[18] the visible absorption spectrum of deoxy Mb appeared, while these reducing agents conventionally afford oxy Mb. In addition,

(26) Alben, J. O.; Fager, L. Y. *Biochemistry* **1972**, *11*, 842–847.

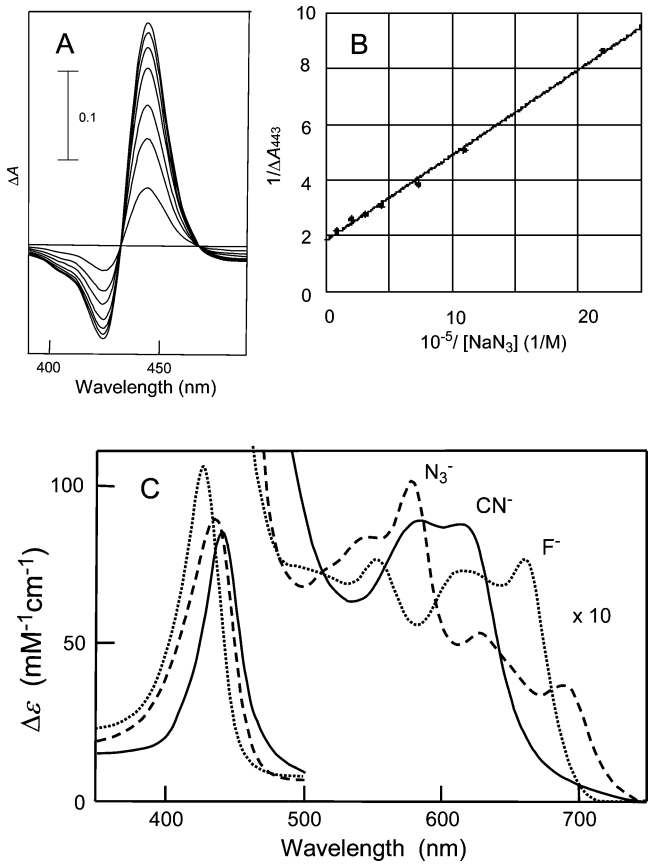

Figure 4. Optical titration of NaN_3 to the ferric Mb containing OxyPyPFe(III). (A) Soret absorption changes in 0.1 M Tris at pH 7.0 and 20 °C over $[NaN_3] = 0-12.3$ mM. (B) Analysis of the absorption changes at 443 nm afforded $K = 6.16 \times 10^5$ M^{-1}. (C) Visible absorption spectra of the azide (---), cyanide (———), and fluoride (••••) derivatives in 0.1 M Tris at pH 7.0 and 20 °C.

Table 1. Visible Absorption Spectra of the Mb Reconstituted with Iron OxyPyP in 0.1 M Tris/HCl at pH 7.0 and 20 °C

ligand	λ_{max}, nm (ε, mM^{-1} cm^{-1})					K^a
			Ferric Derivatives			
none[b]	429 (93.0)	544 (8.0)	610 (7.2)	657 (7.6)		
N_3^-	435 (89.5)	547 (8.4)	577 (10.2)	628 (5.4)	690 (3.7)	1.61×10^5
CN^-	441 (85.4)	585 (8.9)	614 (8.8)			2.10×10^5
F^-	428 (98.7)	510 (6.5)	553 (7.1)	615 (6.8)	661 (7.2)	2.55×10^3
OCN^-	434 (102.4)	542 (6.1)	577 (8.3)	629 (4.4)	689 (3.3)	1.01×10^4
SCN^-	435 (96.4)	547 (7.9)	587 (9.4)	637 (3.2)	701 (2.3)	2.93×10^3
			Ferrous Derivatives			
deoxy	440 (88.6)	457 (77.0)	530sh (4.4)	575 (6.7)	620 (13.4)	
CO	436 (95.3)	460sh (40.2)	582 (7.9)	622 (14.9)		9.94×10^3

[a] Ligand binding constant in M^{-1}. [b] Ferric Mb without exogenous ligand is five-coordinate.

the visible absorption spectrum of the deoxy Mb was invariant up to 760 mmHg of partial oxygen pressure. In other words, even a partial oxygenation was not achieved under pure O_2.

Discussion

Axial Coordination Structure of the Ferric Myoglobin. The 1:1 binding stoichiometry between apoMb and OxyPyPFe(III) suggests the formation of holoprotein. The IR spectral similarity between the ferric azide Mb and the six-coordinate model compound OxyPyPFe(III)•N_3^-•1-MeIm (Figure 5) is consistent with the F8-histidine being

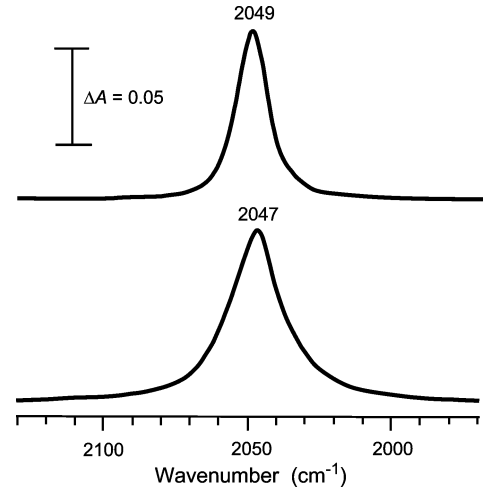

Figure 5. IR spectra of the azide complex of the ferric Mb containing OxyPyPFe(III) in 0.1 M Tris at pH 7.0 and 20 °C (lower), and the mixed-ligand model compound OxyPyPFe(III)N_3^-/1-methylimidazole in chloroform (upper). The iron concentration is 1 mM at 20 °C.

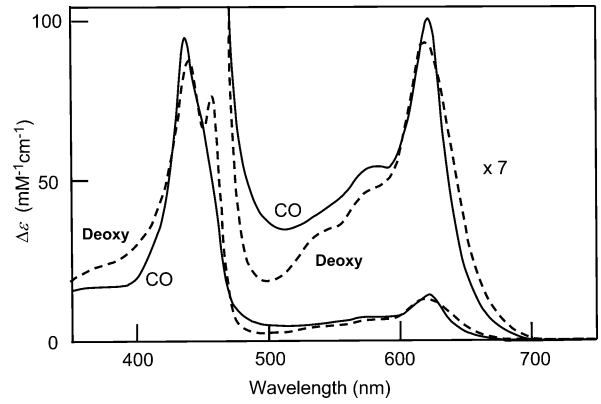

Figure 6. Visible absorption spectra of the ferrous deoxy (---) and CO (———) complexes of the Mb containing OxyPyPFe(II) in 0.1 M Tris at pH 7.0 and 20 °C. The CO concentration is 1 mM.

the proximal ligand. The ligation of the proximal histidine is not surprising because 1-MeIm has a high affinity of $K_1K_2 = 1.16 \times 10^6$ M^{-2} to OxyPyPFe(III) (Figure 2). It is to be noted that the IR absorption band is broader in the Mb (21 cm^{-1}) than in the model (14 cm^{-1}). The broader band for the Mb suggests that the azide interacts with the surrounding globin to adopt several orientations[30] and supports the incorporation of OxyPyPFe(III) into the heme pocket.

It is also notable that the reconstituted ferric Mb in the absence of exogenous ligands does not display the acid−alkaline transitions. The result infers that the iron is six-coordinate with the iron-bound distal imidazole, or that it is five-coordinate without a coordinating water molecule. The former possibility is unlikely because the anionic ligands such as N_3^- and CN^- bind to the Mb with high affinities (Table 1). In addition, the EPR spectrum of the ferric Mb in Figure 3 differs from that of OxyPyPFe(III)•bis(1-MeIm).[10] The EPR spectrum in Figure 3 suggests the high-spin ($S = 5/2$) state for Fe(III). These results, taken together, indicate that the Mb reconstituted with OxyPyPFe(III) is five-coordinate. This is in contrast with six-coordinate native ferric Mb with an iron-bound water. It could be considered that the five-coordinate structure in the Mb may arise from structural

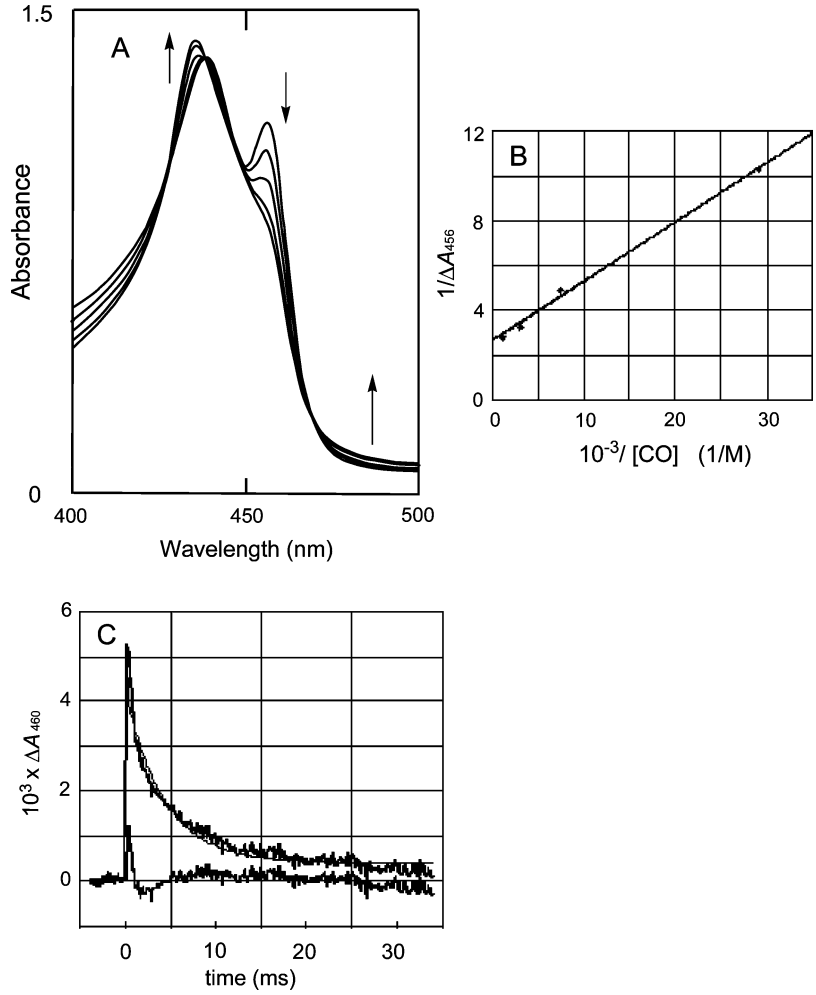

Figure 7. Optical titration of CO to the ferrous Mb reconstituted with OxyPyPFe(II). (A) Soret absorption transition in 0.1 M Tris at pH 7.0 and 20 °C. [CO] = 0−0.96 mM. (B) Analysis of the 456 nm absorption changes afforded $K = 9.94 \times 10^3\ M^{-1}$. (C) Absorption decay of CO rebinding to the Mb after laser photolysis in 0.1 M Tris at pH 7.0 and 20 °C. The bottom trace represents the residual calculated with the observed and theoretical curves.

changes in the surrounding globin after the insertion of unnatural OxyPyPFe(III). This possibility is unlikely because apoMb accommodates various synthetic hemes without significant structural changes of globin.[31,32] The five-coordination of the ferric Mb rather is ascribed to the characteristic coordination structure in OxyPyP.

Functional Anomaly. The most unusual feature of the Mb containing OxyPyPFe(II) is the extreme insensitivity to O_2 and the very low affinity to CO. The Mb exhibits the lowest O_2 and CO affinities among the Mb's known to date.[29] It may be considered that the unusual low reactivity comes from occupation of the iron sixth site by the distal imidazole in the ferrous state. However, the distal histidine ligation in the present Mb is ruled out because the deoxy Mb displays a light absorption spectrum which is entirely different from that of OxyPyPFe(II)·bis(1-MeIm).

The oxygen affinity of Mb generally depends on the pK_3 value of porphyrin, where pK_3 denotes the protonation constant for the core nitrogens, and the oxygen affinity decreases with decreasing pK_3.[33] The pK_3 of 3.9 for OxyPyP is indeed lower than the pK_3 of 4.8 for protoporphyrin but comparable with the pK_3 of 3.7 for the monoformyl porphyrins.[33] Accordingly, it is reasonably assumed that the missing O_2 affinity in deoxy OxyPyPFe(II)−Mb reflects the low pK_3. However, OxyPyP−Mb ($P_{50} \gg 760$ mmHg) exhibits much lower oxygen affinity than the Mb with monoformyl heme ($P_{50} = 1.0-2.7$ mmHg).[33] This observation suggests the presence of another factor to control the oxygen affinity of OxyPyP−Mb.

Structural Mechanism of Ligand Control. Relatively bulky pyridine in the OxyPyP ring widens and deforms the N_4 coordination hole, as evidenced by the EPR spectrum (Figure 3). The functional anomaly of deoxy OxyPyP−Mb is likely to reflect primarily the in-plane distortion of the iron ligand field. The optimized structure of OxyPyP in Figure 1 indicates that the Fe−N(pyridine) bond (2.297 Å)

(27) Neya, S.; Tsubaki, M.; Hori, H.; Yonetani, T.; Funasaki, N. *Inorg. Chem.* **2001**, *40*, 1220–1225.
(28) Neya, S.; Chang, C. K.; Hoshino, T.; Hata, M.; Funasaki, N. *Inorg. Chem.* **2005**, *44*, 1193–1195.
(29) Springer, B. A.; Sliger, S. G.; Olson, J. S.; Phillips, G. N. *Chem. Rev.* **1994**, *94*, 699–714.
(30) Bogumil, R.; Hunter, C. L.; Maurus, R.; Tang, H.-L.; Lee, H.; Lloyd, E.; Brayer, G. D.; Smith, M.; Mauk, A. G. *Biochemistry* **1994**, *33*, 7600–7608.
(31) Sato, T.; Tanaka, N.; Moriyama, H.; Matsumoto, O.; Takenaka, A.; Neya, S.; Funasaki, N. *Bull. Chem. Soc. Jpn.* **1992**, *65*, 739–745.
(32) Neya, S.; Funasaki, N.; Sato, T.; Igarashi, N.; Tanaka, N. *J. Biol. Chem.* **1993**, *268*, 8935–8942.

is much longer than the normal Fe−N(pyrrole) bonds (2.06−2.09 Å) in high-spin Fe(III) porphyrin.[21] The in-plane equilibrium position of the iron atom in the deformed core could be destabilized by the binding of the proximal histidine. In other words, the iron atom in OxyPyP is apt to be pulled up by the proximal base.

Support for the iron displacement comes from the 1-MeIm binding to the model complex. Figure 2 shows that the mono-1-MeIm species accumulates during the 1-MeIm titration. Since accumulation of the monoadduct is correlated with the out-of-plane displacement of the Fe(III),[23] the dominant formation of the mono-1-MeIm complex (Figure 2) indicates that the Fe(III) atom is easily displaced from the OxyPyP plane by the binding of a single 1-MeIm. More support for the facile Fe(III) displacement comes from the IR observation for the azide Mb and the model complex. The IR spectra in Figure 5 show that the spin equilibrium between the $S = 1/2$ and 5/2 states is completely biased toward the high-spin side in the two systems. The high-spin bias is achieved by a large Fe(III) displacement from the macrocycle, and hence by the stabilization of the $d_{x^2-y^2}$ orbital in Fe(III). The third support for Fe(III) displacement comes from the five-coordination state of the ferric Mb. It is to be remembered that the ferric Mb is five-coordinate high-spin with the unusual property of not binding water. The observation indicates that the proximal histidine pulls the Fe(III) from the deformed macrocycle plane. The iron displacement by the proximal histidine is so large that weakly coordinating water does not bind to the iron. It is to be noted that imidazole, which is another neutral ligand, also does not coordinate to the ferric Mb. In the case of anionic ligands such as CN^-, N_3^-, and F^-, however, binding to the positively charged Fe(III) is electrostatic by nature, and these anions regularly coordinate to the Mb. The electron withdrawal by the oxygen atom on the pyridine ring could place a more positive charge on the Fe(III) to enhance the electrostatic iron−anion interactions.

A large iron displacement by the proximal histidine seems significant in the ferrous Mb as well. The gaseous ligands of O_2 and CO coordinate to native Mb with moderate and high affinities, respectively. When the proximal histidine pulls up the Fe(II) atom from the OxyPyP plane, the trans Fe−CO and Fe−O_2 interactions are likely to be much weakened. The kinetic experiment in Figure 7 demonstrates that the k_{off} constant increased by 1080-fold while the k_{on} rate is comparable with that of native Mb with protoheme.[29] It is worthy to point out that reduction of the CO equilibrium affinity primarily comes from the increase in the dissociation rate. The predominant increase in the dissociation rate for CO is consistent with the weakening of the Fe−CO bond due to the an enhanced Fe(II) displacement toward the proximal histidine. A closely related reduction in the equilibrium affinities of O_2 and CO associated with the N_4-core deformation has been reported for the corrphycene-substituted Mb.[34,35]

Biological Relevance. It is to be noted that OxyPyP−Mb shares common coordination properties with a heme enzyme, guanylate cyclase.[36] The protein catalyzes the cyclization of guanosine 5′-triphosphate to guanosine 3′,5′-cyclic monophosphate. The enzyme purified from bovine lungs is five-coordinate in both ferric and ferrous states. The ferrous protein binds CO only weakly and does not react with oxygen.[37] These properties are different from those of native Mb despite the presence of protoheme. The present Mb containing iron OxyPyP is correlated to the enzyme in that the iron is five-coordinate in the ferric and ferrous states, and that it weakly reacts with CO without affinity to O_2. The anomalies in bovine guanylate cyclase have not been explained.[37] According to the crystal structure of the oxygen-binding heme domain of a bacterial guanylate cyclase, the protoheme is highly nonplanar.[38] The nonplanar heme deformation found in the bacterial enzyme is reasonably assumed for the same enzyme from bovines. Although OxyPyP is dissimilar to protoheme, the observation for the OxyPyP-reconstituted Mb may have implications in the reactivity of guanylate cyclase.[37] The highly distorted protoheme in the bovine enzyme is likely to unfavorably accommodate the iron atom, and the iron−porphyrin interactions could be seriously perturbed to reduce the affinity to O_2 and H_2O, as observed for the iron in OxyPyP. Since the crystallographic structures of the five-coordinate guanylate cyclase from bovines are presently unavailable, this hypothesis is still to be verified. Our results at least suggest a possibility that the direct perturbation to the iron placed in a deformed porphyrin core results in a marked reactivity decrease of hemoprotein against the exogenous ligands.

Acknowledgment. We thank Professor Takashi Yonetani, University of Pennsylvania, for helpful discussions. This work was supported by the Japanese Society for the Promotion of Science for Basic Research (Grant Number 18590094).

IC801406X

(33) Sono, M.; Asakura, T. *J. Biol. Chem.* **1975**, *250*, 5227–5232.
(34) Neya, S.; Funasaki, N.; Hori, H.; Imai, K.; Nagatomo, S.; Iwase, T.; Yonetani, T. *Chem. Lett.* **1999**, *28*, 989–990.
(35) Neya, S.; Nakamura, M.; Imai, K.; Funasaki, N. *Chem. Pharm. Bull.* **2001**, *49*, 345–346.
(36) Kasarikov, D. N.; Young, P.; Uversky, V. N.; Garber, N. C. *Arch. Biochem. Biophys.* **2001**, *388*, 185–197.
(37) Stone, J. R.; Marletta, M. A. *Biochemistry* **1994**, *33*, 5636–5640.
(38) Pellicena, P.; Karow, D. S.; Boon, E. M.; Marletta, M. A.; Kuriyan, K. *Proc. Natl. Acad. Sci. U. S. A.* **2004**, *101*, 12854–12859.